Tuning the magnetic anisotropy of Co nanoparticles by metal capping

F. Luis[1], F. Bartolomé[1], F. Petroff[2,3], J. Bartolomé[1], L. M. García[1],
C. Deranlot[2,3], H. Jaffrès[2,3], M. J. Martínez[1], P. Bencok[4],
F. Wilhelm[4], A. Rogalev[4] and N. B. Brookes[4]

[1] *Instituto de Ciencia de Materiales de Aragón, CSIC-Universidad de Zaragoza and Departamento de Física de la Materia Condensada, Universidad de Zaragoza 50009 Zaragoza, Spain*
[2] *Unité Mixte de Physique CNRS/Thales - Route Départementale 128 91767 Palaiseau Cedex, France*
[3] *Université Paris-Sud - 91405 Orsay Cedex, France*
[4] *European Synchrotron Radiation Facility - BP 220, F-38043 Grenoble, France*

Abstract. – The magnetic anisotropy of Co clusters with diameters ranging from 1.1 nm to 4.5 nm turns out to be significantly larger than in bulk and strongly increasing with decreasing cluster size. The dominating role of the surface can be used to modify the anisotropy by changing the electronic properties of the matrix surrounding the clusters. We find that capping the clusters by a metallic (Cu and Au) layer significantly enhances the anisotropy, thus also stabilizing the magnetization against thermal fluctuations. The observed anisotropy enhancement is attributed to the bonding of the Co $3d$ electrons to the conduction band of the capping layer, which depends on the electronic band structures of both metals.

Metal films and nanoparticles show fascinating size effects stemming from the electronic localization and the symmetry breaking at the surface. The large fraction of surface atoms in very thin Co films generates a strong magnetic anisotropy perpendicular to the film plane [1], which results from the incomplete quenching and the anisotropy of their orbital magnetic moments m_L [2]. A similarly enhanced anisotropy occurs in Co 2-d mono-atomic layer islands deposited on Pt [3–5]. Three-dimensional clusters consist of core atoms, with nearly bulk properties [6], surrounded by a shell of surface atoms in direct contact with either vacuum or a matrix. The increase of the surface to volume ratio leads to the increase of the anisotropy constant K with decreasing cluster size [7–10].

For very small clusters, magnetic properties become dominated by the properties of surface atoms [9]. It is then logical that K is affected by the interaction of these atoms with their surroundings. This effect has been observed for thin films, whose anisotropy and magnetization depend strongly on the type of substrate on which they grow [11,12]. For clusters, however, a clear-cut assessment of how the matrix modifies the anisotropy is still lacking, mainly because the disparity of preparation methods and substrates prevents a direct comparison.

In this letter, we show that a new family of Co granular layers might overcome this difficulty. The preparation method described below enables us to modify the interface between
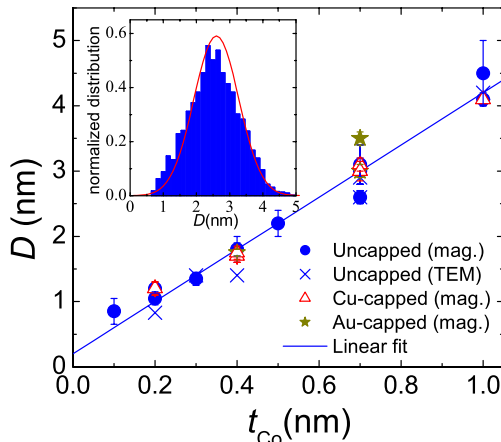
Fig. 1 – (Color online) Dependence of the average cluster size on the nominal thickness of deposited Co. Data obtained from TEM ($\times$) and from magnetization fits are shown. Inset: size distribution obtained from the fit of magnetic data (solid line) and from TEM pictures (histogram) for a Co/Al_2O_3 sample with $t_{Co} = 0.7$ nm.

the clusters and their surroundings while keeping all the other structural and geometrical parameters constant. We have compared the magnetization dynamics and the anisotropy of clusters embedded in alumina with those of clusters capped by a thin noble metal (Cu or Au) layer. Capping leads to a significant enhancement of the surface anisotropy, being much larger for Au than for Cu. This phenomenon is attributed to the hybridization of the $3d$ electrons of surface Co atoms with the conduction bands of Cu or Au. Nanometer-sized Co clusters were prepared by sequential sputter deposition of Al_2O_3 and Co layers on a Si substrate as described elsewhere [13,14]. The Co layer forms spherical fcc metal clusters. Their average diameter D increases linearly with the thickness t_{Co} that the deposits would have if they were continuous (see fig. 1). The size distribution has been determined from TEM and magnetic measurements. Results obtained by the two methods on samples prepared simultaneously agree very well (see the inset of fig. 1) [9,13]. For the same t_{Co}, different preparation runs lead to slightly different D values. The distribution is approximately Gaussian, with a rather narrow width $\sigma \simeq (0.2$–$0.3)D$. The analysis of EXAFS spectra reveals a contraction of the clusters' lattice similar to that observed for free clusters, suggesting strain to be weak. Within each layer, clusters are homogeneously dispersed, separated by a nearly constant distance of ~ 2.2 nm. A fraction x_{para} (< 0.4 in the present samples) of the deposited Co is not visible as clusters in TEM pictures. It is attributed to the presence of single atoms or very small clusters, made of two or three atoms, embedded in the Al_2O_3 matrix. Capped clusters can be easily prepared by depositing a 1.5 nm thick layer of a noble metal M (Cu or Au) onto the preformed clusters. We do not expect the crystal structure and morphology of the clusters to be affected by the capping. In fact, D values agree well with those of clusters in alumina. In the case of Au [15], we observe that magnetic properties are independent of the thickness of the capping layer, between 1.5 and 6 nm. Samples are usually made by piling up a number N of these Co/Al_2O_3 or $Co/M/Al_2O_3$ repetition units.

The ac susceptibility χ and magnetization M were measured using a commercial SQUID
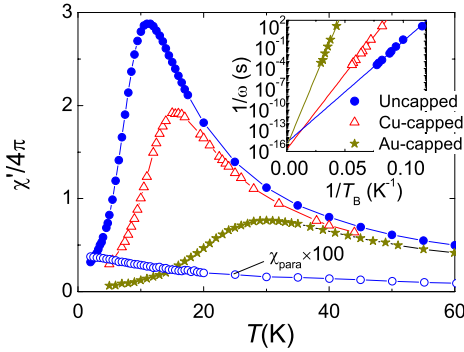
Fig. 2

Fig. 3

Fig. 2 – (Color online) Ac susceptibility of Co clusters (in SI units per unit of Co volume) either uncapped or capped by Cu and Au measured at $\omega/2\pi = 10$ Hz. The three samples have $N = 25$ layers and average $D = 1.8(1)$, $1.75(5)$, and $1.75(5)$ nm, respectively. Also shown ($\circ$) is a magnification of the susceptibility of the fraction ($x_{\text{para}} \simeq 0.2$ for the three samples) of non-aggregated Co atoms present in the $Al_2O_3/Co/Al_2O_3$ multilayer. It was obtained from the magnetization measured at $B = 5$ T. Inset: Arrhenius plots for the same samples. Blocking temperatures were obtained from ac χ' and dc susceptibility measurements performed after cooling at zero field.
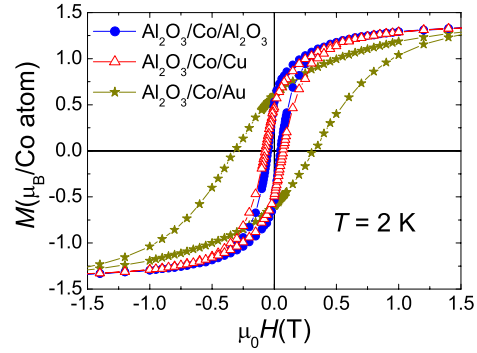
Fig. 3 – (Color online) Magnetization hysteresis loops of the same samples.

magnetometer. The diamagnetic signal from a bare silicon substrate was measured and adequately subtracted from all experimental data. The contribution of the x_{para} fraction has been separated from that of the nanoparticles by studying high-field ($B = 5$ T) magnetization curves measured over a broad temperature range ($1.8\,\text{K} < T < 300\,\text{K}$) [9]. As shown in fig. 2, it is completely negligible with respect to χ of the nanoparticles in the temperature region of interest. X-ray Magnetic Circular Dichroism (XMCD) experiments were performed on the same samples at relevant absorption edges: $L_{2,3}$ edges of Co, using total electron yield detection in normal incidence geometry to avoid self-absorption effects; K edges of Co and Cu and $L_{2,3}$ edges of Au, with total fluorescence yield detection in backscattering geometry.

The anisotropy determines the rate at which magnetic moments flip: K times the cluster volume V gives the energy barrier U for the thermally activated magnetization reversal. The relaxation time is given by Arrhenius' law

$$\tau = \tau_0 \exp\left[\frac{U}{k_{\text{B}}T}\right]. \tag{1}$$

Quantitative information on U and K can be obtained from χ vs. T data, like those shown in fig. 2. Deviations from the Curie-Weiss equilibrium behavior occur as T decreases since τ becomes exponentially longer. Near the so-called superparamagnetic blocking temperature T_{b}, where the typical relaxation time becomes of order $1/\omega$, the in-phase susceptibility χ' drops abruptly. The variation of T_{b} with frequency, which follows also Arrhenius' law as shown in the inset of fig. 2, provides then a direct measure of the anisotropy strength. In fig. 2 we compare χ and T_{b} measured on clusters embedded in alumina or capped by either Cu or Au. The average cluster magnetic moments and the size distributions are very similar for the three samples (compare the susceptibilities measured above T_{b}). In spite of this, T_{b} of the sample with Cu is about 40 % larger than that of the clusters embedded in alumina whereas

for Au, T_b increases by nearly a factor 3. Capping the clusters has the effect of increasing the effective U, stabilizing the magnetization against thermal fluctuations. A similar *qualitative* conclusion can be drawn from magnetization hysteresis loops measured in the frozen magnetic state ($T < T_b$), which are shown in fig. 3. The capping makes the loops significantly broader: for $D = 1.8\,\mathrm{nm}$, the coercive field $\mu_0 H_c$ increases from $50\,\mathrm{mT}$ for clusters in alumina to $73\,\mathrm{mT}$ for Cu-capped clusters and to $320\,\mathrm{mT}$ for Au-capped clusters. These data indicate that capping with a noble metal makes the clusters magnetically harder.

The same trend is observed for samples with varying D. For $D > 2\,\mathrm{nm}$, measurements were performed on single layers to avoid dipolar inter-layer interactions [16]. In order to take into account the cluster's size distribution, we performed a scaling analysis [9] of the out-of-phase susceptibility χ''. This component is nearly proportional to the distribution of U in a given sample. Knowing the distributions of D and U enables us to accurately determine the effective K. This method neglects the variation of K with temperature in the neighborhood of T_b. This variation, which has been observed for magnetic nanoparticles [17], is expected to be weak in the case of Co, whose Curie temperature is very high [18]. In fig. 4 we plot K of uncapped and capped clusters as a function of D. In agreement with previous results [9], K largely exceeds the bulk value for fcc Co [18] and increases as D decreases. This size dependence indicates that K is enhanced at the cluster surface. Separation between surface and core atoms has proven useful to understand the electronic structure of Co and other fcc metal (Au, Pt) clusters [6]. Within this simple core-shell picture K is described by

$$K = f K_{\mathrm{surface}} + (1 - f) K_{\mathrm{bulk}}, \qquad (2)$$

where K_{surface} refers to surface atoms, $K_{\mathrm{bulk}} = 7 \times 10^4\,\mathrm{J/m^3}$ is the contribution arising from the bulk anisotropy of fcc Co [18] and $f \simeq 1 - (1 - a/D)^3$, with $a = 0.4\,\mathrm{nm}$, is the fraction of surface atoms in a fcc cluster. For the smallest clusters ($1\,\mathrm{nm}$), nearly 80 % of the atoms (of order 55) lie at the cluster's interface with the surrounding matrix. This simple model (solid lines in fig. 4) enables us to get an estimate for K_{surface} and to study how it is modified by the capping. For uncapped clusters, $K_{\mathrm{surface}} \simeq 25 K_{\mathrm{bulk}}$. For Cu-capped clusters, $K_{\mathrm{surface}} \simeq 40 K_{\mathrm{bulk}}$, *i.e.* about 60 % larger than for clusters in pure alumina, whereas capping with Au makes it almost three times larger ($K_{\mathrm{surface}} \sim 70 K_{\mathrm{bulk}}$).

The dependence of K_{surface} on the surrounding material is reminiscent of the behavior observed for thin Co films. Films sandwiched by Cu have a larger perpendicular surface anisotropy (of about $0.15(4)\,\mathrm{mJ/m^2}$) than uncapped Cu/Co films [19]. For Au/Co/Au films the anisotropy is even stronger, $0.6\text{–}0.7(3)\,\mathrm{mJ/m^2}$ [20, 21], and dominates over the shape anisotropy for less than eleven atomic layers. The same qualitative trend is followed by the anisotropy per unit of surface $(K_{\mathrm{surface}} - K_{\mathrm{bulk}})Df/6 = 0.33$, 0.53 and $0.97\,\mathrm{mJ/m^2}$ (or, equivalently, 0.13, 0.21, and $0.38\,\mathrm{meV}$ per surface atom) that we obtain for clusters in alumina, capped by Cu and by Au, respectively. Clusters have different surface atomic sites (located at the corners, edges or face centers) that might have different electronic properties and interactions with the capping metal. These details could explain why the simple eq. (2) fails to quantitatively account for the size-dependent K of Au-capped clusters. Unfortunately, *ab initio* calculations of K have been performed for bare fcc Co clusters only [22]. Here we content ourselves with a qualitative analysis, in analogy with models developed for thin films. On the basis of *ab initio* electronic band calculations [23–25], the anisotropy induced by the capping was attributed to the hybridization of the $3d$ electronic states of Co with the conduction band of Cu and Au. The out-of-plane Co d-orbitals overlap with the capping metal d-orbitals at the interface, broadening this band with respect to the band generated by the in-plane Co-Co bonds [25]. As a consequence the orbital moment component perpendicular to
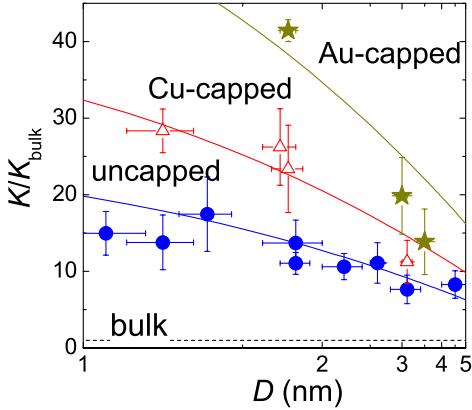
Fig. 4

Fig. 5

Fig. 4 – (Color online) Average magnetic anisotropy normalized to its bulk value $K_{\text{bulk}} = 7 \times 10^4 \, \text{J/m}^3$ [18], as a function of cluster diameter for Al_2O_3/Co, $Al_2O_3/Co/Cu$, and $Al_2O_3/Co/Au$ layers. Solid lines are least-square fits of a core-shell model (see eq. (2)) to the data.
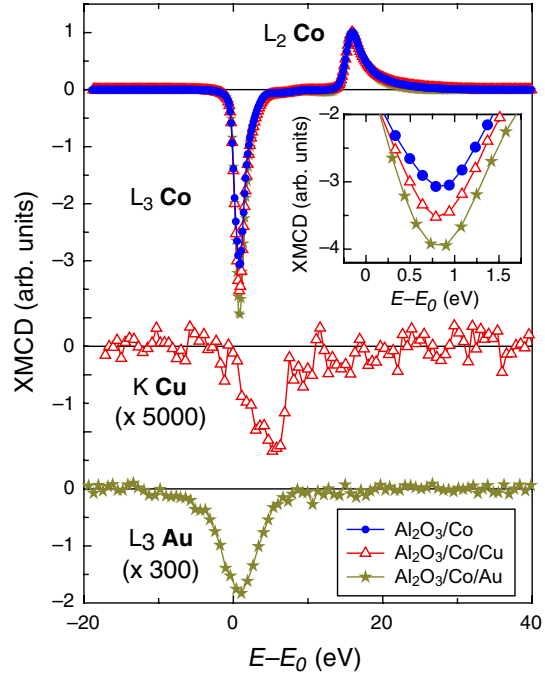
Fig. 5 – (Color online) XMCD spectra obtained at $T = 5 \, \text{K}$ and under an applied magnetic field of 1 T of several Al_2O_3/Co, $Al_2O_3/Co/Cu$, and $Al_2O_3/Co/Au$ granular multilayers with $t_{\text{Co}} = 0.7 \, \text{nm}$. The Co - $L_{2,3}$ XMCD data are shown in the upper plot. To emphasize the changes induced by metal capping, they are normalized to the height of the L_2 peak. The inset shows a detail of the L_3 edge region. XMCD signals near the Au - L_3 and Cu-K edges are shown in the medium and lower plots, respectively. The origin of the energy scale is taken at the inflection point of the adequate absorption edges.

the interface increases. The magnetocrystalline anisotropy increases then, since it arises from the difference between the spin-orbit energies for the spin parallel and perpendicular to the particle surface. The fact that Au induces a larger anisotropy can be explained by the smaller difference between the energies of the unoccupied d-orbitals of Co and Au, which leads to a stronger bonding [23].

This interpretation is supported by the XMCD data of fig. 5. The presence of a noble-metal overlayer clearly increases the ratio between the L_3 and L_2 XMCD peaks of Co. Applying the XMCD sum rules, we find that the ratio m_L/m_S of orbital to spin magnetic moments increases from 0.13(1) for the uncapped clusters to 0.16(1) and 0.20(1) for, respectively, Cu- and Au-capped clusters, all larger than the bulk 0.08(1) [26] and showing the same qualitative trend as the anisotropy. We refrain here from giving m_L and m_S values because the number n_{h} of d-electron holes is not well known in nanoparticles and can depend on size. On the other hand, the ratio m_L/m_S is independent of n_{h}. The value found for the Cu-capped sample agrees well with $m_L/m_S = 0.16(4)$ found Co clusters of similar size prepared in a copper matrix [27]. Interpolating data of Dürr $et\ al.$ [28] for disk-like Co clusters supported

on a Au(111) surface, we get $m_L/m_S = 0.19(2)$ for clusters of 2000 atoms, also in very good agreement with our data. The agreement between data obtained for samples prepared by different methods suggests that the enhancement of the orbital magnetism by the capping is an intrinsic electronic effect associated with the interaction between Co and the noble metal layer. In addition, the enhancement seems to be larger in nanoparticles than in thin films. Indeed, m_L/m_S has been found to be ≤ 0.12 for both Cu/Co [26] and Au/Co/Au films [20].

Despite the enhancement of the orbital magnetism, susceptibility and magnetization experiments (see figs. 2 and 3, and fig. 1 in [15]) show that the net cluster magnetic moments remain virtually unaltered after capping, at least within a few percent. This result vividly contrasts with the quenching of magnetism observed in Co clusters prepared by co-depositing Co and a Cu matrix [29]. A plausible explanation is that our method prevents the intermixing and alloying of Co and Cu, which is known to cause a significant reduction of the Co magnetic moments [29, 30].

Evidences for the hybridization at the interface are also provided by absorption spectra of Cu and Au, which show XMCD signals near their K and L_3 absorption edges, respectively. Their signs show that the *s-p* and *d* bands of Cu and Au, respectively, are ferromagnetically polarized by the corresponding electrons of Co. The polarization of the Cu *s-p* band, of order $0.02\mu_B$ per atom [31], is similar to that observed in Co/Cu multilayers [32]. For the $5d$ Au electrons, we find $m_L/m_S = 0.20(2)$, which is of the same sign but somewhat larger than the value $m_L/m_S = 0.12(2)$ found in the case of Au/Co/Au multilayers [33]. Again, this polarization does not appreciably change the effective magnetic moment per particle but probably plays an important role in determining the anisotropy.

Polarization of Au and Cu electronic spins by Co can also mediate RKKY interactions between neighbor magnetic particles [29]. We may argue, however, that interactions are not the dominant source of the observed anisotropy enhancement. The correlation we observe between K and m_L is typical of systems with strong surface anisotropy [2, 3, 20, 25]. The size-dependence of τ_0 and of the Weiss temperature, determined by fitting Curie-Weiss' law to the equilibrium χ, suggest that interaction effects become stronger with increasing size, whereas capping effects on K become larger for smaller particles (fig. 4). Furthermore, the contribution of interactions to U can be suppressed by applying relatively weak magnetic fields [34, 35]. By contrast, hysteresis loops (fig. 3) and χ'' data show that the anisotropy enhancement persists under external magnetic fields. Finally, Cu is expected to give rise to stronger interactions than Au [36], again in contradiction with the stronger anisotropy found for Au-capped clusters.

Concluding, despite the important differences in morphology that exist between two-dimensional films or disks and fcc clusters, the anisotropic bonding to a noble metal overlayer leads to qualitatively the same effect. This suggests that the anisotropy is mainly determined by the electronic states of the two metals [23]. Therefore, we expect that the interface anisotropy could be tuned by choosing materials with appropriate electronic band structures.

$* * *$

REFERENCES

[1] Chappert C., Le Dang K., Beauvillain P., Hurdequint H. and Renard D., *Phys. Rev. B*, **34** (1986) 3192.

[2]   BRUNO P., *Phys. Rev. B*, **39** (1989) R865.
[3]   GAMBARDELLA P. *et al.*, *Science*, **300** (2003) 1130.
[4]   RUSPONI S., CREN T., WEISS N., EPPLE M., BULUSCHEK P., CLAUDE L. and BRUNE H., *Nature Mater.*, **2** (2003) 546.
[5]   BANSMANN J. *et al.*, *Surf. Sci. Rep.*, **56** (2005) 189.
[6]   PAULUS P. M., GOOSSENS A., THIEL R., VAN DER KRAAN A., SCHMID G. and DE JONGH L. J., *Phys. Rev. B*, **64** (2001) 205418.
[7]   BØDKER F., MØRUP S. and LINDEROTH S., *Phys. Rev. Lett.*, **72** (1994) 282.
[8]   RESPAUD M. *et al.*, *Phys. Rev. B*, **57** (1998) 2925.
[9]   LUIS F. *et al.*, *Phys. Rev. B*, **65** (2002) 094409.
[10] JAMET M., WERNSDORFER W., THIRION CH., DUPUIS V., MÉLINON P., PÉREZ A. and MAILLY D., *Phys. Rev. B*, **69** (2004) 024401.
[11] DEN BROEDER F. J. A., HOVING W. and BLOEMEN P. H. J., *J. Magn. & Magn. Mater.*, **93** (1991) 562.
[12] WILHELM F. *et al.*, *J. Magn. & Magn. Mater.*, **222** (2000) 163.
[13] MAURICE J. L., BRIÁTICO J., CARREY J., PETROFF F., SCHELP L. F. and VAURÈS A., *Philos. Mag. A*, **79** (1999) 2921.
[14] BRIÁTICO J., MAURICE J. L., CARREY J., IMHOFF D., PETROFF F. and VAURÈS A., *Eur. Phys. J. D*, **9** (1999) 517.
[15] LUIS F. *et al.*, *J. Appl. Phys.*, **99** (2006) 08G705.
[16] LUIS F., PETROFF F., TORRES J. M., GARCÍA L. M., BARTOLOMÉ J., CARREY J. and VAURÈS A., *Phys. Rev. Lett.*, **88** (2002) 217205.
[17] ANTONIAK C., LINDNER J. and FARLE M., *Europhys. Lett.*, **70** (2004) 250.
[18] SUCKSMITH W. A. and THOMPSON J. E., *Proc. R. Soc. London*, **225** (1954) 362.
[19] KRAMS P., LAUKS F., STAMPS R. L., HILLEBRANDS B. and GÜNTHERODT G., *Phys. Rev. Lett.*, **69** (1992) 3674.
[20] WELLER D. *et al.*, *Phys. Rev. Lett.*, **75** (1995) 3752.
[21] KISIELEWSKI M., MAZIEWSKI A., TEKIELAK M., WAWRO A. and BACZEWSKI L. T., *Phys. Rev. Lett.*, **89** (2002) 087203.
[22] XIE Y. and BLACKMAN J. A., *J. Phys.: Condens. Matter*, **16** (2004) 3163.
[23] WANG D., WU R. and FREEMAN A. J., *J. Magn. & Magn. Mater.*, **129** (1994) 237.
[24] UJFALUSSY B., SZUNYOGH L., BRUNO P. and WEINBERGER P., *Phys. Rev. Lett.*, **77** (1996) 1805.
[25] STÖHR J., *J. Magn. & Magn. Mater.*, **200** (1999) 470.
[26] TISCHER M. *et al.*, *Phys. Rev. Lett.*, **75** (1995) 1602.
[27] EASTHAM D. A. AND KIRKAM I. W., *J. Phys.: Condens. Matter*, **12** (2000) L525.
[28] DÜRR H. A., DHESI S. S., DUDZIK E., KNABBEN D., VAN DER LAAN G., GOEDKOOP J. B. and HILLEBRECHT F. U., *Phys. Rev. B*, **59** (1999) R701.
[29] QIANG Y., SABIRYANOV R. F., JASWAL S. S., LIU Y., HABERLAND H. and SELLMYER D. J., *Phys. Rev. B*, **66** (2002) 064404; EASTHAM D. A., QIANG Y., MADDOCK H., KRAFT J., SCHILLE J. P., THOMPSON G. S. and HABERLAND H., *J. Phys.: Condens. Matter*, **9** (1997) L497.
[30] XIE Y. and BLACKMAN J. A., *Phys. Rev. B*, **66** (2002) 155417.
[31] GARCÍA L. M. *et al.*, to be published in *J. Magn. & Magn. Mater.*
[32] PIZZINI S., FONTAINE A., GIORGETTI C., DARTYGE E., BOBO J. F., PIECUCH M. and BAUDELET F., *Phys. Rev. Lett.*, **74** (1995) 1470.
[33] WILHELM F. *et al.*, *Phys. Rev. B*, **69** (2004) 220404(R).
[34] NORDBLAD P., JÖNSSON P. E., FELTON S., SVEDLINDH P. and HANSEN M. F., *Phys. Rev. B*, **64** (2001) 212402.
[35] LUIS F., BARTOLOMÉ J. and PETROFF F., *J. Phys.: Condens. Matter*, **16** (2004) 5109.
[36] BRUNO P. and CHAPPERT C., *Phys. Rev. Lett.*, **67** (1991) 1602.